Determination of channel interaction in barium for five $5d\,7d$ perturbers: The $^1D_2$, $^3F_2$, $^1P_1$, $^3S_1$, and $^3P_0$ states

Oliver C. Mullins, Yifu Zhu, and T. F. Gallagher
Department of Physics, University of Virginia, Charlottesville, Virginia 22901
(Received 31 January 1985)

The measurement of the interaction in barium of five bound, doubly excited perturber states with singly excited Rydberg series is reported. The five perturbers are the $5d\,7d\,^1D_2$, $5d\,7d\,^3F_2$, $5d\,7d\,^1P_1$, $5d\,7d\,^3S_1$, and $5d\,7d\,^3P_0$ states. The $J=2$ perturbers interact with the $6snd\,^3D_2$ and $6snd\,^1D_2$ Rydberg series; the $J=1$ perturbers interact with the $6snd\,^3D_1$ and $6sns\,^3S_1$ series; and the $J=0$ perturber interacts with the $6sns\,^1S_0$ series. We observe the relative cross section for photoexcitation of the $6p\,7d$ autoionizing resonance from each of the perturbers and interacting states nearby in energy where the photon energy roughly corresponds to the energy separation of the $5d$ and $6p$ Ba^+ states. The relative strength of the transition is directly related to the $5d\,7d$ character of the bound states. Good agreement with extensive previous work is obtained for the $5d\,7d\,^1D_2$ and $5d\,7d\,^3P_0$ states. General agreement with previous work is obtained for the $5d\,7d\,^3F_2$, $5d\,7d\,^1P_1$, and $5d\,7d\,^3S_1$ states and specific discrepancies are clarified.

I. INTRODUCTION

In barium a relatively large number of doubly excited states, in which two electrons possess excitation energy, exist below the first ionization limit and represent members of Rydberg series which converge to higher ionization limits. These states or "perturbers" interact with Rydberg series which converge to the first ionization limit thereby producing perturbations in the energies and other properties of these Rydberg series. Energy-level analyses of the interacting states performed, for instance, with the methods of multichannel quantum-defect theory[1–3] (MQDT) provide predictions of the strength of interaction and of the state wave functions which are linear combinations of Rydberg and perturber wave functions.[4–7] Generally, the energy-level studies treat a large number of states but are subject to some uncertainty because significant changes in atomic wave functions are not always accompanied by significant energy-level shifts. The study of a variety of effects has been used to probe bound-state wave functions including Stark shifts,[8,9] hyperfine splittings,[10] g factors,[11] radiative decay measurements,[8,12,13] multiphoton ionization methods,[14] photoelectron spectroscopy[15–19] (PES), and isotope shifts.[20]

Here, we report the use of a novel approach to measure the perturber character of members of perturbed Rydberg series using photoexcitation to specific autoionizing resonances. The method is straightforward in principle and in practice and yields data which require little analysis to yield significant results. In this paper we describe the principles of the method, our experimental approach, and the results for five barium $5d\,7d$ perturbers of the term symbols; $^1D_2$, $^3F_2$, $^1P_1$, $^3S_1$, and $^3P_0$.

II. PRINCIPLES OF THE METHOD

The bound-state wavefunctions ψ_B can be represented as linear combinations of Rydberg (ψ_R) and perturber (ψ_p) wave functions. We consider a two-channel case for simplicity where the Rydberg wave function is of the form $6snl$ ($n \geq 13$):

$$\psi_B = Z_R \psi_R + Z_p \psi_p \ , \tag{1}$$

where the Z_i's are the respective coefficients of the basis functions from each of the two collision channels of quantum-defect theory. The standard convention of a unit norm is assumed for the basis functions and state wave functions so that the sum of the squares of the Z coefficients equals 1 (as defined in Ref. 4 and references therein). With this normalization, the ratio of the squared coefficients can be considered to represent the ratio of time the wave function spends in each of the basis states. If the basis functions are normalized per unit energy (see Ref. 2) then the coefficients represent the ratio of the number of orbits for each of the basis functions representing the wave function.[21]

Now let us consider the photoionization of a state with the wave function given by Eq. (1) by a photon of energy such that the final energy equals that of the autoionizing $6p\,7d$ state. In Fig. 1 we show the possible excitation processes for the $6snl$ and the $5d\,7d$ parts of the wave function where we have assumed that there is no mixing of the $5d\,7d$ and $6snl$ states for clarity. As shown by Fig. 1, the four possible excitations consist of two excitations to the continua and two excitations to the autoionizing $6p\,7d$ state. The strengths of these processes may be estimated in a straightforward way. The estimated photoionization cross sections for the direct process[22] are found to be quite small; for the process $5d\,7d + h\nu \rightarrow 5d + \epsilon$, $\sigma \sim 10^{-18}$ cm^2 and for the process $6s\,20d + h\nu \rightarrow 6s + \epsilon$, $\sigma \sim 10^{-19}$ cm^2. The cross section for excitation of the $6p\,7d$ state from the $5d\,7d$ state is essentially the cross section for the strong Ba^+ $5d \rightarrow 6p$ transition spread over the width of the $6p\,7d$ state, 280 cm^{-1}, where the $7d$ electron is a spectator.[23–25] The estimate[26] for this cross section is $\sim 10^{-15}$ cm^2. The

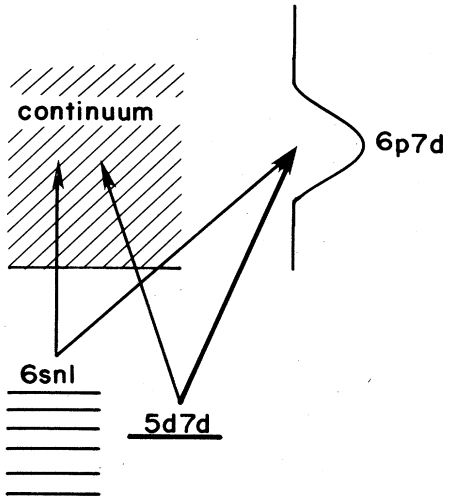

FIG. 1. Schematic diagram of the possible photoexcitation processes from $6snl$ and $5d7d$ states to the energy of the autoionizing $6p7d$ state. At energies relevant to this work the continuum consists of both the $6s$ and $5d$ states of Ba^+.

$6snl+h\nu\rightarrow 6p7d$ cross section consists of the strong Ba^+ $6s\rightarrow 6p$ transition reduced by the square of the overlap integral between the nl and $7d$ electrons. For $l\neq 2$ the overlap integral is zero and for $l=2$ the estimated cross section is $\sim 10^{-18}$ cm^2.

Although our estimates for different photoionization processes are approximate, it is clear that the dominant process is $5d7d+h\nu\rightarrow 6p7d$. Thus the photoionization cross section σ_B of a bound state is dominated by this process which depends only on the $5d7d$ character of the wave function, and we may ignore all other processes. In this approximation σ_B is given by

$$\sigma_B = Z_p^2 \sigma_p \ , \tag{2}$$

where σ_p is the $5d7d\rightarrow 6p7d$ cross section, $\sim 10^{-15}$ cm^2. Thus, as stated above, by measuring the relative photoionization cross sections σ_B we obtain directly the perturber character Z_p^2. This is in principle, and in practice, a very unambiguous means of determining the perturber character of bound states.

III. APPARATUS AND PROCEDURES

In order to prepare and photoionize states of interest, the second and third harmonics of a Nd:YAG (YAG denotes yttrium aluminum garnet) laser were used to pump three or four tunable dye lasers as needed. The laser polarizations were chosen to enhance the production of desired bound states (collinear polarizations for $J=0,2$ states and crossed linear polarizations for $J=1$ states). The laser which photoexcited the $6p7d$ autoionizing resonance was linearly polarized. The laser pulses intersected an atomic beam of barium sequentially in time ($\Delta t\sim 6$ ns) in the order corresponding to their excitations. The interaction region was located between two plates, one with a grid, $1\frac{1}{2}$ cm apart such that the ions could be collected by application to one plate of an appropriate voltage ($\sim$400 V) 150 ns after photoionization. Application of a significantly larger voltage ($\sim$4000 V) to the plate resulted in field ionization of atomic states of a sufficiently large principal quantum number ($n>20$). This method was applied only for the $5d7d\ ^1D_2$ experiment; another technique was required for lower-lying states. The analog signal from a venetian blind particle detector was time gated with a boxcar integrator and recorded on an X-Y plotter.

For the study of all five perturbers, the bound, even-parity states were formed with two tunable lasers, the first exciting atoms to the $6s6p\ ^1P_1^0$ state and the second exciting atoms from the $^1P_1^0$ state to the desired state (see Fig. 2). A third tunable laser was employed to photoexcite the even-parity states to a $6p7d$ autoionizing resonance. Care was taken to keep the photoionization signal linear in the power of the third laser.

First, a suitable $6p7d$ autoionizing resonance was located by setting the second laser wavelength to excite a state with substantial $5d7d$ character and then scanning the third laser wavelength in the vicinity of the Ba^+ $5d\rightarrow 6p$ transitions. In all cases a prominent resonance was found at 57 840 cm^{-1} and corresponds to two superimposed resonances of $J=1$ and 3. (The locations of the $J=2$ resonances were not determined explicitly.) Additionally, this resonance was produced by photoexciting the $6s7d\ ^1D_2$ state with a laser whose frequency corresponded to the Ba^+ $6s\rightarrow 6p$ transition. Figure 3 shows the $J=1$ $6p7d$ resonance at 57 840 cm^{-1}; this figure shows the ion signal for the photoionization of the $5d7d\ ^3P_0$ state as a func-

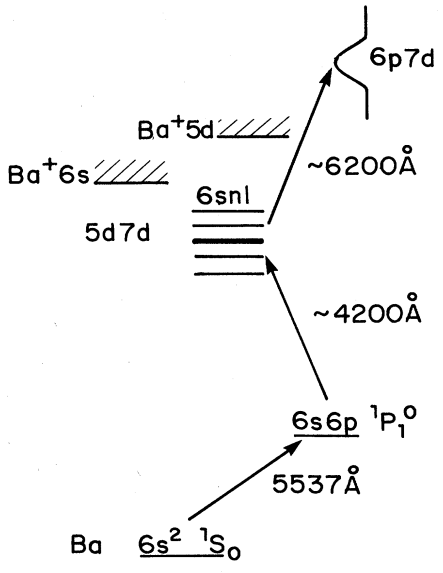

FIG. 2. Relevant energy levels for our experiments. The three photoexcitation steps are shown which resulted in the production of the $6p7d$ autoionizing resonance from different even-parity bound states.

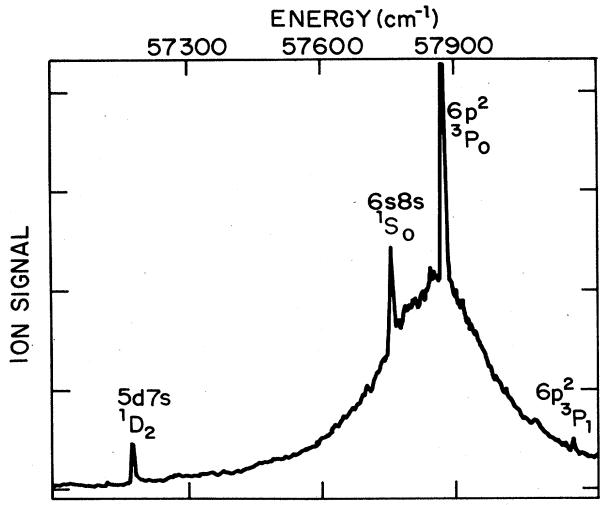

FIG. 3. $6p\,7d$ autoionizing resonance. The ion signal is recorded on a linear scale as a function of the frequency of the ionizing (third) laser. The first two lasers are set to populate the $5d\,7d\ ^3P_0$ state. Sharp features correspond to the excitation of bound states (from the $6s\,6p\ ^1P_1^0$ state) and photoionization both performed by the scanning third laser. Note that the $6p\,7d$ autoionizing resonance is $\sim 280\ \mathrm{cm}^{-1}$ wide.

tion of the ionizing laser frequency. The sharp features correspond to excitation of bound states from the $6s\,6p\ ^1P_1^0$ state and photoionization, both performed by the third laser, and serve as frequency markers. Note that the full width at half maximum of the autoionizing resonance is $280\ \mathrm{cm}^{-1}$.

Having located an appropriate $6p\,7d$ autoionizing state we then proceeded to measure the relative photoexcitation cross section to the $6p\,7d$ state. This was done in two steps.

First, the ion signal corresponding to the photoexcitation cross section of the $6p\,7d$ resonance from the various bound states was obtained by fixing the frequency of the ionizing laser and scanning the second laser [see (a) panels in Figs. 4—8] which photoexcites bound states from the $6s\,6p\ ^1P_1^0$ state. Different final-state energies result from this method but this does not materially affect the observed photoionization signal, especially for the few states that interact most strongly because the autoionization resonance is so wide in energy. One exception will be discussed later.

Second, we measured the excitation probabilities of the bound states by scanning the second laser thereby producing the different bound states and then ionizing these states with 100% efficiency. (We shall return to how we accomplished this shortly.) The excitation spectra so obtained are shown in Figs. 4—8 [(b) panels].

To obtain the relative photoexcitation cross sections of bound states to the $6p\,7d$ state from the spectra of Figs. 4—8 [(a) panels], we must take into account the different

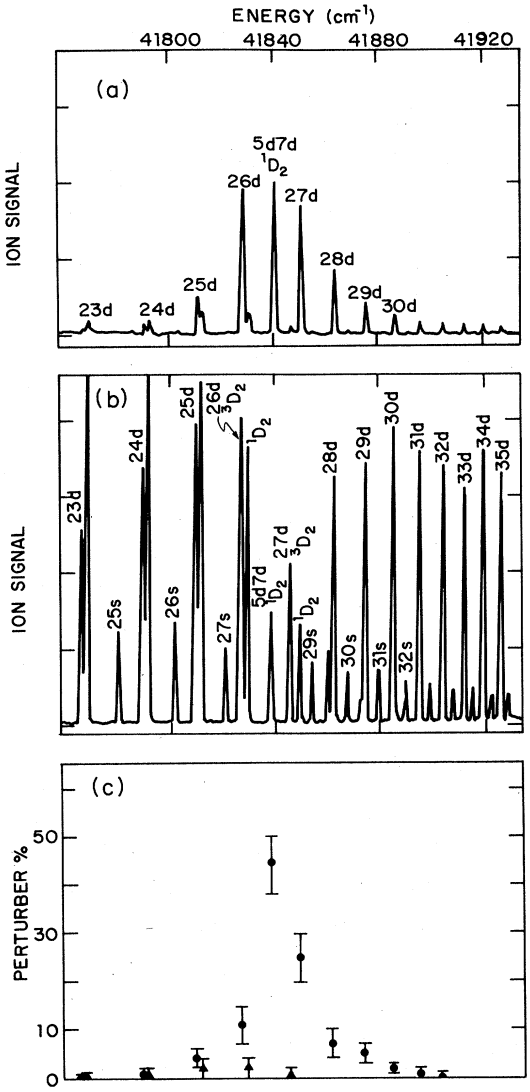

FIG. 4. $5d\,7d\ ^1D_2$ perturber. (a) shows the ion signal recorded as the second laser is scanned thereby exciting the $6s\,6p\ ^1P_1^0$ to the $5d\,7d\ ^1D_2$ perturber and nearby states. The third laser frequency is fixed so as to excite the perturber and nearby states to the $6p\,7d$ autoionizing resonance shown in Fig. 4. The ion signal was maintained linear in the power of the third laser. (b) shows the relative cross section for formation of the perturber and nearby states in our experiment. The ion signal was collected as the second laser was scanned and the states excited were ionized with 100% efficiency by field ionization. $^3D_2$ states are slightly displaced to lower energy from the $^1D_2$ states and the $^1S_0$ states are smaller peaks roughly midway between adjacent D_2 peaks. Note that the $5d\,7d\ ^1D_2$ and $6s\,28s\ ^1S_0$ peaks are superimposed. (c) depicts the perturber character which is proportional to the relative cross section for formation of the $6p\,7d$ autoionizing resonance for these states. This figure was obtained by normalizing the trace of (a) by that of (b) with appropriate modifications discussed in the text. ●, the perturbed branch of the Lu-Fano plot; ▲, the unperturbed branch (see Ref. 5).

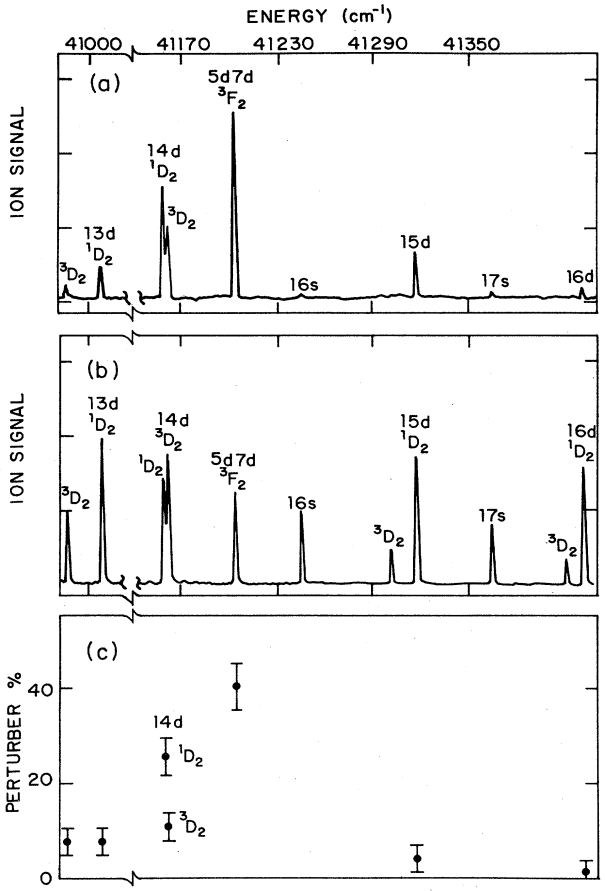

FIG. 5. $5d7d\ ^3F_2$ perturber. (a) shows the ion signal recorded as the second laser is scanned thereby exciting the $6s6p\ ^1P_1^0$ state to the $5d7d\ ^3F_2$ perturber and nearby states. The third laser frequency is fixed so as to excite the $6p7d$ autoionizing resonance. Note the break in the x axis; the scale is the same on both sides of the break. (b) shows the relative cross section for formation of the perturber and nearby states in our experiment. The ion signal was collected as the second laser was scanned and states excited were photoionized with 100% efficiency as described in the text. (c) depicts the perturber character which is proportional to the relative cross section for formation of the $6p7d$ autoionizing resonance for these states. To obtain (c) a trace similar to (a) was used [normalized by (b)] except that the third laser frequency was adjusted to keep the total energy of the three-photon process constant. Adjusting the ionizing laser frequency was done for this case because the interacting states span an energy difference greater than the $6p7d$ autoionizing width; only the (small) calculated fraction of the $13d$ mixing was appreciably affected by altering the ionizing laser frequency vs leaving it fixed.

probabilities of formation of the various bound states. This we do by dividing the peak heights for each interacting bound state in Fig. 4(a) by the peak height of the same state in Fig. 4(b), etc. The resulting ratios are proportional to σ_B or to Z_p^2. In Figs. 4—8 [(c) panels] we plot the ratios as Z_p^2 with the normalization condition that $\sum Z_p^2 = 1$. The data plotted in Figs. 4—8 [(c) panels] represent average values obtained in replicate runs.

Let us now consider details which are peculiar to the study of specific perturbers. For the $5d7d\ ^1D_2$ perturber and interacting states, field ionization was used to record the excitation spectrum of Fig. 4(b). The field ionization pulse was applied 150 ns after the arrival of the second laser pulse. Because the various states have quite different

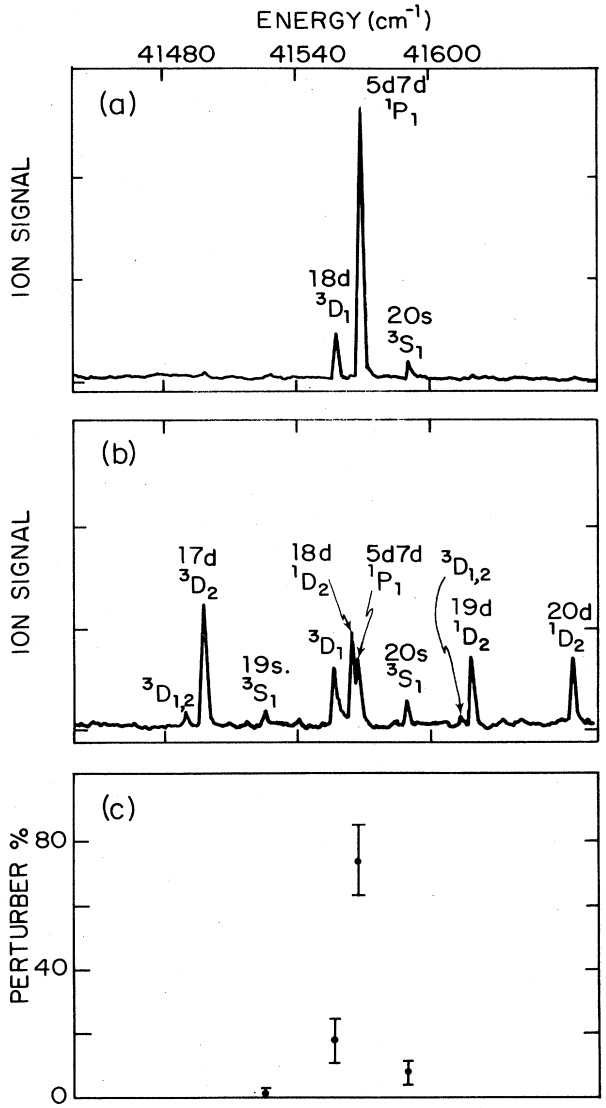

FIG. 6. $5d7d\ ^1P_1$ perturber. (a) shows the ion signal recorded as the second laser is scanned thereby exciting the $6s6p\ ^1P_1^0$ state to the $5d7d\ ^1P_1$ perturber and nearby states. The third laser frequency is fixed so as to excite the $6p7d$ autoionizing resonance. (b) shows the relative cross section for formation of the perturber and nearby states in our experiment. The ion signal was collected as the second laser was scanned and the states excited were photoionized with 100% efficiency. (c) depicts the perturber character which is proportional to the relative cross section for formation of the $6p7d$ autoionizing resonance for these states. To obtain (c), the trace of (a) was normalized by that of (b).

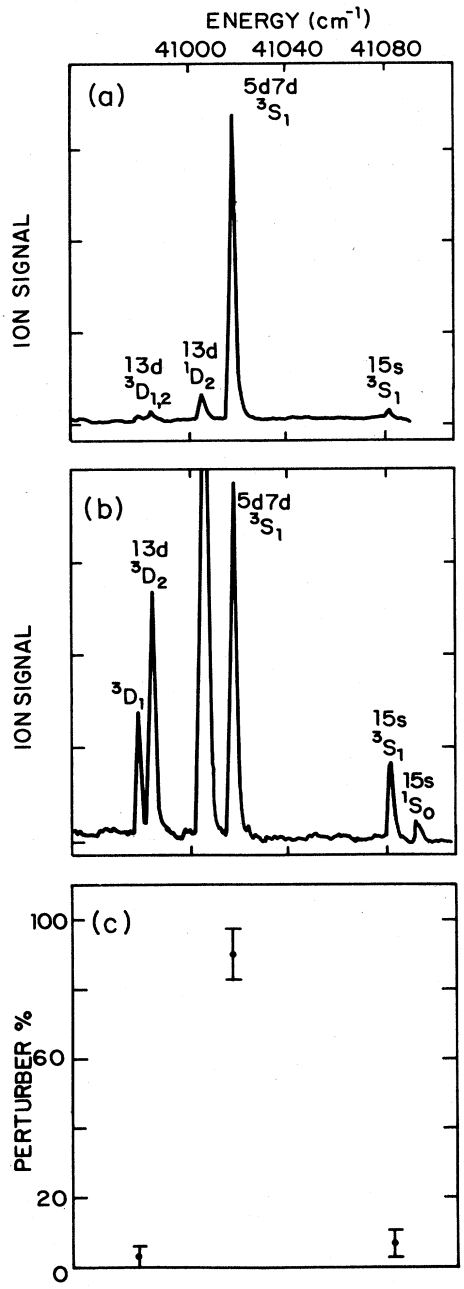

FIG. 7. $5d7d\ ^3S_1$ perturber. (a) shows the ion signal recorded as the second laser is scanned thereby exciting the $6s6p\ ^1P_1^0$ state to the $5d7d\ ^3S_1$ perturber and nearby states. The third laser frequency is fixed so as to excite the $6p7d$ autoionizing resonance. (b) shows the relative cross section for formation of the perturber and nearby states in our experiment. The ion signal was collected as the second laser was scanned and the states excited were photoionized with 100% efficiency. (c) depicts the perturber character which is proportional to the relative cross section for formation of the $6p7d$ autoionizing resonance for these states. To obtain (c) the trace of (a) was normalized by that of (b).

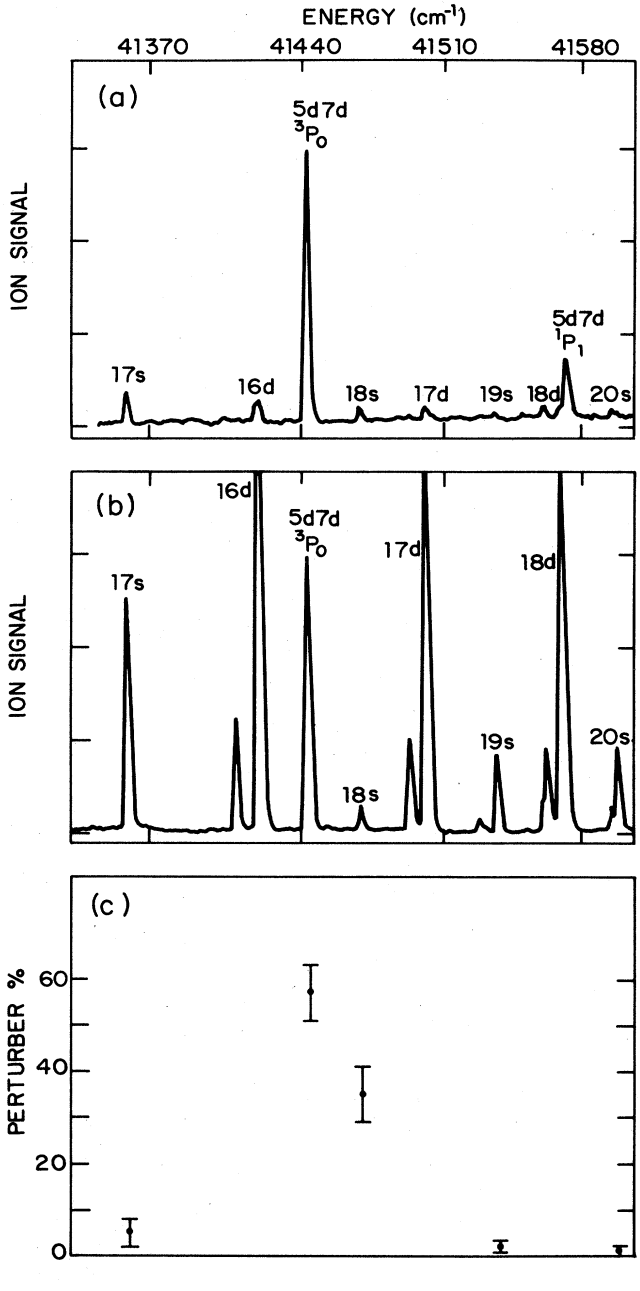

FIG. 8. $5d7d\ ^3P_0$ perturber. (a) shows the ion signal recorded as the second laser is scanned thereby exciting the $6s6p\ ^1P_1^0$ state to the $5d7d\ ^3P_0$ perturber and nearby states. The third laser frequency is fixed so as to excite the $6p7d$ autoionizing resonance. Note that the $5d7d\ ^1P_1$ perturber appears in this scan in spite of the collinear polarizations of the first two lasers. See Fig. 6 for the analysis of this perturber. (b) shows the relative cross section for formation of the perturber and nearby states in our experiment. The ion signal was collected as the second laser was scanned and the states excited were photoionized with 100% efficiency. (c) depicts the perturber character which is proportional to the relative cross section for formation of the $6p7d$ autoionizing resonance for these states. To obtain (c) the trace of (a) was normalized by that of (b).

lifetimes it was necessary to extrapolate back to zero time with known radiative decay constants[8] to determine atomic state populations. Blackbody-radiation-induced excitation-field ionization[27] produced a significant ionization signal, especially for the states of large principal quantum numbers n; this background was subtracted from Fig. 4(a) for the preparation of Fig. 4(c).

For the lower-lying perturbers field ionization is more difficult so the excitation spectra of Figs. 5—8 [(b) panels] were obtained by photoionization using a fourth dye laser tuned to the Ba^+ $6s_{1/2} \rightarrow 6p_{3/2}$ transition.[23–25] This transition which can easily be saturated results in the 100% conversion of bound $6snl$ states to autoionizing $6pnl$ states.

As we noted above, the $6p\,7d$ autoionizing state is so wide compared to the range covered by the interacting Rydberg states around a $5d\,7d$ perturber that we could safely leave the third laser wavelength fixed. This approximation begins to break down in the study of the lowest-lying perturber, the $5d\,7d\ ^3F_2$ state. For this state the energy range scanned by the second laser is large, $\sim 400\ cm^{-1}$, so an additional experiment was performed in which the frequency of the ionization laser was adjusted so that the same final-state energy was obtained in the photoionization of all the states; these data were used to construct Fig. 5(c). The differences were small (except for the larger perturber character for the $6s\,13d$ states for a constant final energy); thus we are assured that the errors for the higher-lying perturbers are negligible.

IV. RESULTS AND DISCUSSION

As discussed earlier for each of the perturbers and interacting states the relative cross sections or Z_p^2 coefficients for formation of the $6p\,7d$ resonance (Figs. 4—8) were obtained by normalizing the photoexcitation scans for forming the $6p\,7d$ autoionizing resonance [Figs. 4—8, (a) panels] by the photoexcitation scans for forming the bound states [Figs. 4—8, (b) panels] with appropriate modifications discussed in Sec. III. The cross section for photoexcitation of the $6p\,7d$ resonance from the states investigated is in all five cases dominated by the $5d\,7d$ character of the bound state. This is perhaps most evident for the $5d\,7d\ ^3P_0$ perturber shown in Fig. 8. The bound-state excitation scan [Fig. 8(b)] shows that the production of the $6snd\ ^1D_2$ dominates the production of $6sns\ ^1S_0$ states. Nevertheless, the photoionization scan corresponding to the production of the $6p\,7d$ autoionizing resonance [Fig. 8(a)] is dominated by the $5d\,7d\ ^3P_0$ state with the $^1D_2$ states appearing as very small peaks.

In each of the five cases the state which has previously been labeled the perturber is the state which we find to have the greatest perturber character.[5–7]

For the $5d\,7d\ ^1D_2$ state our results are in good agreement with an MQDT energy-level analysis,[5] a state-lifetime analysis,[8] and a photoelectron spectroscopic (PES) analysis.[15] The $5d7d\ ^1D_2$ state is found to interact with the nominal triplets of lower energy and singlets of higher energy. The nature of this interaction has recently been described within the framework of an MQDT analysis.[28]

For the $5d\,7d\ ^3P_0$ state our results are again in good agreement with previous work including an MQDT energy level analysis,[7] a state-lifetime analysis,[12] an isotope-shift analysis,[20] and an PES study.[16] The $5d\,7d\ ^3P_0$ state is found to interact primarily with the $6s\,18s\ ^1S_0$ state and to a much smaller extent the $6s\,17s\ ^1S_0$ state.

For the $5d\,7d\ ^3F_2$ state, our data clarifies a discrepancy in the literature. Several methods have shown the strong interaction between the $5d\,7d\ ^3F_2$ state and the $6s\,14d\ ^1D_2$ state. However, disagreement exists concerning the extent of mixing between the $6s\,14d\ ^3D_2$ and the $5d\,7d\ ^3F_2$ state. Our results show that the $5d7d\ ^3F_2$ state mixes strongly with the $6s\,14d\ ^1D_2$ state and to a lesser but significant extent with the $6s\,14d\ ^3D_2$ state [higher-resolution scans than Figs. 5(a) and 5(b) clearly show the $6s\,14d\ ^3D_2$ interaction]. Lifetime measurements[13] support the finding of the strong $6s\,14d\ ^3D_2$ interaction with the perturber. Additionally, it has recently been shown that the singlet-triplet mixing for the $6s\,14d\ ^{1,3}D_2$ states is both substantial and considerably larger than for other $6snd$ states for $n \sim 14$.[29] The experimental method employed in this study was to observe the relative transition strengths for forming the two $6p_{3/2}nd_j$ $J=3$ autoionizing series from the $6snd\ ^{1,3}D_2$ states for $n=8$—17.[29] The singlet-triplet mixing of the $6s\,14d\ ^{1,3}D_2$ states can be considered to be a two-step process; (i) the $6s\,14d\ ^1D_2$ interacts with and is repelled by the $5d7d\ ^3F_2$ state to an energy nearly degenerate with the $6s\,14d\ ^3D_2$ state, (ii) the $6s\,14d\ ^{1,3}D_2$ states interact and repel each other. In step (i) the $6s\,14d\ ^1D_2$ state acquires substantial $5d\,7d\ ^3F_2$ character so in step (ii) the $6s\,14d\ ^3D_2$ also acquires $5d7d\ ^3F_2$ character.

Our finding of appreciable mixing of the $6s\,14d\ ^3D_2$ state and perturber is not corroborated by an MQDT analysis of energy-level positions[5] nor by the isotope-shift measurements.[20] We note that the determination of the perturber character by measuring relative isotope shifts is a somewhat less direct method than that employed here. Both the lifetime measurements[13] and the observed singlet-triplet mixing of the $6s\,14d\ ^{1,3}D_2$ states[29] require $6s\,14d\ ^3D_2$ and perturber mixing but these results were not used to obtain mixing coefficients; here we are able to do so.

Additionally, the $6s\,13d$ states show perturber character but this may be due to interaction with a perturber which we have not studied, the $5d\,7d\ ^3D_2$ state which is located between the $6s\,12d$ and $6s\,13d$ states.

The $5d\,7d\ ^1P_1$ and $5d\,7d\ ^3S_1$ states have not been the subject of extensive study as some of the $J=0,2$ $5d\,7d$ perturbers but an energy level analysis has been performed.[6] Generally, our results, that these two perturbers are not strongly mixed with the $6snl$ Rydberg series, are consistent with the energy level analysis.[6] Our results clearly indicate some mixing of the $5d\,7d\ ^1P_1$ state with the $6s\,18d\ ^3D_1$ state and to a lesser extent with the $6s20s\ ^3S_1$ state; this interaction can be discerned from the Lu-Fano plot of these states (see Ref. 6).

An enhanced cross section to form $J=1$ bound states occurs near the $5d\,7d\ ^1P_1$ perturber. The bound-state excitation scan clearly shows the production of the $5d\,7d\ ^1P_1$ perturber and the $6s\,19s\ ^3S_1$ and $6s\,20s\ ^3S_1$ states while the $6s\,18s\ ^3S_1$ and the $6s\,21s\ ^3S_1$ are not evident. Also, the enhanced production of the $6s\,18d\ ^3D_1$

state is clear. It is quite likely that the enhancement of $J=1$ states near the $5d7d\ ^1P_1^0$ perturber results from channel interaction. This increased cross section for forming the $J=1$ states by photoexciting the $6s6p\ ^1P_1^0$ state results partially from the extensive $5d6p\ ^1P_1^0$ character ($\sim 40\%$) of the $6s6p\ ^1P_1^0$ state[30] and partially from the fact that the excitation of the Rydberg parts of the $J=1$ states is spin forbidden. The fact that the relative cross sections for excitations of the $J=1$ states is not in direct proportion to their perturber character implies that appreciable interference may exist for exciting the doubly excited versus Rydberg character of these states. The observation of this kind of interference has been described for the photoexcitation of the $6s6p\ ^1P_1^0$ state to $J=0$ states near the $5d7d\ ^3P_0$ perturber [see Fig. 8(b)].[16]

It is encouraging that the dominant channel interactions we report here are in agreement with previous findings, in particular with energy-level analyses. However, we point out that when the interactions and thus energy-level shifts are small, then the results of energy-level analyses should be regarded with caution. For these cases probes of state wave functions are required which are more sensitive to the channel interaction.

ACKNOWLEDGMENTS

This work has been supported by the National Science Foundation Grant No. PHY-84-19357.

[1]M. J. Seaton, Proc. Phys. Soc. London **88**, 801 (1966).
[2]U. Fano, Phys. Rev. A **2**, 353 (1970).
[3]K. T. Lu, Phys. Rev. A **4**, 579 (1971).
[4]J. A. Armstrong, P. Esherick, and J. J. Wynne, Phys. Rev. A **15**, 180 (1977).
[5]M. Aymar and O. Robaux, J. Phys. B **12**, 531 (1979).
[6]M. Aymar and P. Camus, Phys. Rev. A **28**, 850 (1983); also see P. Camus, M. Dieulin, and A. El Himdy, *ibid.* **26**, 379 (1982).
[7]M. Aymar, P. Camus, M. Dieulin, and C. Morillon, Phys. Rev. A **18**, 2173 (1978).
[8]T. F. Gallagher, W. Sandner, and K. A. Safinya, Phys. Rev. A **23**, 2969 (1981).
[9]R. J. Fonck, F. L. Roesler, D. H. Tracy, K. T. Lu, F. S. Tomkins, and W. R. S. Garton, Phys. Rev. Lett. **39**, 1513 (1977).
[10]R. Beigang, K. Lucke, and A. Timmermann, Phys. Rev. A **27**, 587 (1983).
[11]J. J. Wynne, J. A. Armstrong, and P. Esherick, Phys. Rev. Lett. **39**, 1520 (1977).
[12]M. Aymar, P. Grafstrom, C. Levison, H. Lundberg, and S. Svanberg, J. Phys. B **15**, 877 (1982).
[13]K. Bhatia, P. Grafstrom, C. Levison, H. Lundberg, L. Nilsson, and S. Svanberg, Z. Phys. A **303**, 1 (1981).
[14]S. A. Bhatti, C. L. Cromer, and W. E. Cooke, Phys. Rev. A **24**, 161 (1981).
[15]E. Matthias, P. Zoller, D. S. Elliot, N. D. Piltch, S. J. Smith, and G. Leuchs, Phys. Rev. Lett. **50**, 1914 (1983).
[16]G. Leuchs and S. J. Smith, Phys. Rev. A **31**, 2283 (1985).
[17]O. C. Mullins, R.-l. Chien, J. E. Hunter III, J. S. Keller, and R. S. Berry, Phys. Rev. A **31**, 321 (1985).
[18]O. C. Mullins, R.-l. Chien, J. E. Hunter III, D. K. Jordan, and R. S. Berry, Phys. Rev. A **31**, 3059 (1985).
[19]O. C. Mullins, J. E. Hunter III, J. S. Keller, and R. S. Berry, Phys. Rev. Lett. **54**, 410 (1985).
[20]J. Neukammer, E. Matthias, and H. Rinneberg, Phys. Rev. A **25**, 2426 (1982).
[21]W. E. Cooke and C. L. Cromer (unpublished).
[22]D. C. Lorents, D. J. Eckstrom, and D. Huestis, SRI Report No. MP 73-2, 1973 (unpublished).
[23]W. E. Cooke, T. F. Gallagher, S. A. Edelstein, and R. M. Hill, Phys. Rev. Lett. **40**, 178 (1978).
[24]F. Gounand, T. F. Gallagher, W. Sandner, K. A. Safinya, and R. Kachru, Phys. Rev. A **27**, 1925 (1983).
[25]N. H. Tran, P. Pillet, R. Kachru, and T. F. Gallagher, Phys. Rev. A **29**, 2640 (1984).
[26]A. C. G. Mitchell and M. W. Zemansky, *Resonance Radiation and Excited Atoms* (Cambridge University, London, 1934).
[27]W. E. Cooke and T. F. Gallagher, Phys. Rev. A **21**, 588 (1980).
[28]A. Giusti-Suzor and U. Fano, J. Phys. B **17**, 4277 (1984).
[29]O. C. Mullins, Y. Zhu, E. Y. Xu, and T. F. Gallagher (unpublished).
[30]Y. K. Kim and P. S. Bagus, Phys. Rev. A **8**, 1739 (1973).